

# The Rmodynamic Analysis Of Water Sorption To Ca<sub>4</sub>Na<sub>4</sub>A Zeolitic

Kokhkharov Mirzokhid Xusanboyevich<sup>1</sup>, Oydinov Mukhlis Xoliqul o'g'li<sup>2</sup>, Kuldasheva Shakhnoza Abdulazizovna<sup>3</sup>, Marguba Abdullaeva Tolibjanovna<sup>4</sup>

<sup>1</sup>*Doctor of Philosophy (PhD) in Employee Senior Research, Institute of General and Inorganic Chemistry, Tashkent, Uzbekistan.*

<sup>2</sup>*Intern Researcher, Institute of General and Inorganic Chemistry, Tashkent, Uzbekistan.*

<sup>3</sup>*Doctor of Chemistry, Chief Researcher, Institute of General and Inorganic Chemistry, Tashkent, Uzbekistan*

<sup>4</sup>*Doctor of Philosophy (PhD) in Technical Sciences Toshkent Medical Academy Uzbekistan, Toshkent.*

**Keywords:** *Isotherm, adsorption heat, entropy, thermo kinetics, Ionic molecular complexes, zeolite Ca<sub>4</sub>Na<sub>4</sub>A, H<sub>2</sub>O, adsorption calorimeter.*

**Аннотация.** *The differential heat, isotherm, differential entropy, and term kinetics of carbon dioxide adsorption on Ca<sub>4</sub>Na<sub>4</sub>A zeolite are measure at 303 K. Based on the results obtained, the mechanism of water adsorption in Ca<sub>4</sub>Na<sub>4</sub>A zeolite from initial filling to saturation is described in detail. The adsorption isotherm was described using the MXTN (Theory of volume saturation of micropores equation).*

## 1. INTRODUCTION.

Natural and synthetic zeolites with molecular porosity properties are used widely as adsorbents. Synthetic zeolites are molecularly porous, aluminosilicate, microporous adsorbents, which not only have selective adsorption but also differ in their size and ability to absorb substances. Characterized by a stable crystalline structure and a large surface area. Zeolite pores are spherical cavities connected by canals. At present, industrial enterprises produce different brands of zeolites, which differ in cations and porous sizes. [1]

Zeolites are characterized by a very high rate of moisture assimilation. A high degree of drying is maintained at almost the entire stage. The increase in moisture at the end of the phase makes it important to use solid adsorbents. [2].

The main component of natural gas is methane. Soon, methane will be considered the transitional feedstock in the production of petrochemicals. This includes a decrease in oil reserves, an increase in natural and associated gas reserves, and biogas production, and in particular the production of hydrocarbons such as ethylene and propylene from methane [3].

The fact that the RHO zeolite (Si/Al = 3) is bonded to eight rings (D8R) to form large voids indicates that it is composed of aluminosilicates [3]. In the center of the zeolite, a large cavity is formed in the form of a cubic octahedron [5].

Цеолит структурасини тузилишида β-бўшлиқни ташкил қилган олтига халқа (6R) ва ҳалқаларни туташтириб турувчи тўрт халқали (4R) кублар саккиз халқани (8R), α-катта бўшлиқни ташкил қилади. Каттароқ молекулалар (8R) бўшлиқ орқали ўтиб адсорбцияланади [6-10]. The six-ring (6R) and four-ring (4R) cubes connecting the rings

that form the b-cavity in the zeolite structure form a large eight-ring (8R) cavity. Larger molecules (8R) are adsorbed through the cavity.

The ability of molecules to penetrate pores depends on the type, location, and deformation process of the cations [11-13]. When water molecules are adsorbed, they penetrate the pores of the adsorbent and also help determine the adsorption volume and acidic properties of the adsorbent [14-18]. In the hydrated composition, less conformational changes are observed than in the dehydrated structure of the adsorbent [19]. Due to the hydrophilicity of the RHO zeolite, H<sub>2</sub>O significantly affects the stability of the adsorbent composition [20-22].

The enthalpy of adsorption is determined using calorimetric measurements obtained with a Tian-Calvet calorimeter [23] and the isostatic enthalpy of adsorption.

By studying the adsorption properties of zeolites, their adsorption isotherms, thermodynamic and kinetic functions are determined [24-30].

## 2. RESEARCH METHODS AND OBJECTS.

For microcalorimetric studies, we used a type A synthetic zeolite Ca<sub>4</sub>Na<sub>4</sub>A (Si/Al=1). The composition of the elemental cells of zeolite obtained for the study is Ca<sub>4</sub>Na<sub>4</sub>A - Ca<sub>4</sub>Na<sub>4</sub> [(AlO<sub>2</sub>) 12 (SiO<sub>2</sub>) 12] 27H<sub>2</sub>O. Absolute water was selected for adsorption on Ca<sub>4</sub>Na<sub>4</sub>A zeolite. The Ca<sub>4</sub>Na<sub>4</sub>A zeolite was carried out in a high-vacuum adsorption microcalorimetric device when determining the adsorption of water [31-32].

The adsorbates were first frozen and then purified using a vacuum pump and zeolites. The microcalorimeter allows you to measure the heat energy released over a long period. The determination of adsorption measurements was carried out in a high-vacuum adsorption device and was calculated by the capillary method. Swallowing small amounts of adsorbates increases the accuracy of adsorption measurements.

## 3. RESULTS AND DISCUSSIONS.

The amount of water adsorption ( $N$ ) on the Ca<sub>4</sub>Na<sub>4</sub>A zeolite was expressed in the unit cell of H<sub>2</sub>O, and the pressure isotherm from initial saturation to saturation was expressed in units of  $\ln(p/p^0)$ . In fig. 1 shows the adsorption isotherm ( $\ln$ ) of water adsorption on the Ca<sub>4</sub>Na<sub>4</sub>A zeolite at a temperature of 303 K at a relative pressure of  $\sim 10^{-6} p/p^0$  ( $p$  is the water vapor pressure,  $p^0$  (303K) = 4.42 kPa). The adsorption isotherm was studied in several stages. At the initial stage, the isotherm of water adsorption in the Ca<sub>4</sub>Na<sub>4</sub>A zeolite is primarily equal to  $\ln(p/p^0) = -14.26$ ,  $r=0.0000006344$  millimeters of mercury, and the adsorption value starts from  $N = 0.28$  H<sub>2</sub>O/e.ya. From the small value of the relative pressure, it is known that the water molecule penetrates the micropores of the zeolite. From the small value of the relative pressure, it is known that the water molecule penetrates the micropores of the zeolite.

The adsorption isotherm tends to the adsorption axis in the range from  $\ln(p/p^0) = -14.26$  to  $\ln(p/p^0) = -11.71$ , where the degree of adsorption is  $N = 13.15$  H<sub>2</sub>O/e. Here the adsorption pressure is in the range from  $r=0.0000006344$  mm.Hg to  $r=0.000008215$  mm.Hg. Then the graph of the isotherm partially rises vertically, reaching  $N = 8.35$  H<sub>2</sub>O / eya, and the logarithm of the isotherm is  $\ln(p/p^0) = -10.39$ , where the adsorption pressure is from  $r=0.000008215$  mm.Hg range  $0.00097$  mm.Hg. Phase water molecules with adsorption amount up to  $N = 8.35$  H<sub>2</sub>O / pc. They are firmly attached to the pores of the zeolite, and the adsorbate molecules are inert. The adsorption isotherm then continues, as in the previous stages, and at  $\ln(p/p^0) = -8.65$  relative to the adsorption axis and  $\ln(p/p^0) = -7.56$ , the

isotherm graph rises vertically. At the end of this stage, the adsorption axis tends to  $\ln (p/p^\circ) = - 3.24$  and  $\ln (p/p^\circ) = - 0.65$ , and the adsorption isotherm is vertical at  $\ln (p/p^\circ) = - 0, sixteen$ .

In adsorption processes up to  $\ln (p/p^\circ) = - 3.24$  water molecules form monomeric and dimeric complex compounds with cations  $Ca^{+2}$  and  $Na^+$  in zeolite. Consequently, isotherm values up to this value occur in the order in which the stages of the adsorption process occur. Then water molecules fill the pores of the zeolite, and saturation approaches the vapor pressure.

The adsorption of water in  $Ca_4Na_4A$  molecular sieves was redefined using the three-dimensional equation of the volumetric theory of micropore saturation [33–34].

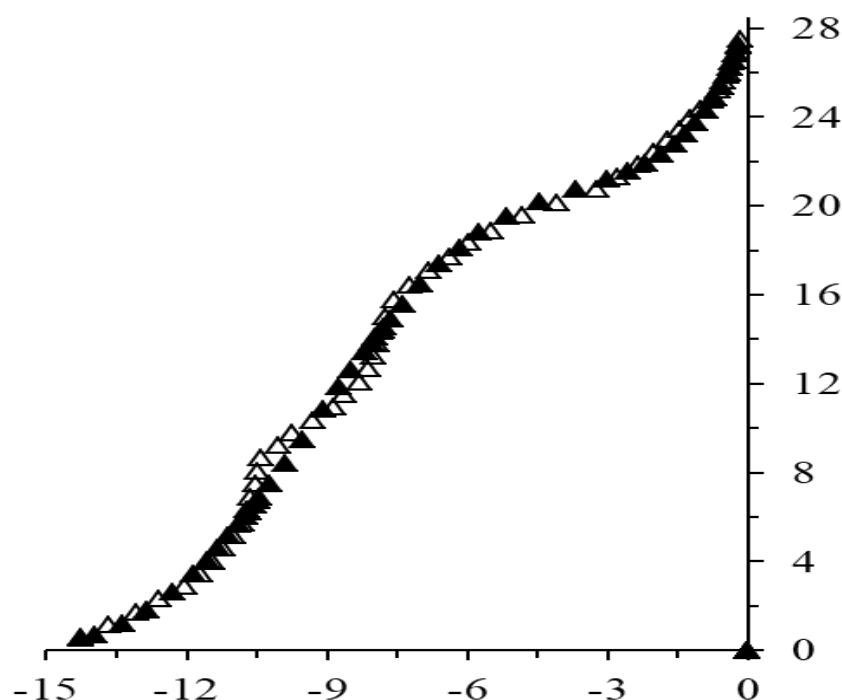


Figure 1. Adsorption value of water adsorption isotherm in zeolite  $Ca_4Na_4A$  at 303 K; Points are calculated using the formula  $\blacktriangle$  -MXTN (Theory of volume saturation of micropores)

$$N = 18,958 \exp[A/26,14]^4 + 1,772 \exp[A/20,17]^5 + 7,555 \exp[A/3,03]^1,$$

Where: N-adsorption in micropores,  $(H_2O)/\text{eya}$ ,  $A = RT \ln (P^\circ/P) - 1 H_2O / \text{eya}$  - work done to transfer steam from the surface (pressure  $P^\circ$ ) to the equilibrium vapor phase (pressure R)

The differential heat of adsorption of water on zeolite  $Ca_4Na_4A$  ( $Q_d$ ) (Fig. 2) is given at a temperature of 303 K. Long lines - heat of condensation of water below 303 K ( $\Delta H_v = 43.5$  kJ/mol). In this zeolite, the heat of adsorption decreases in the form of an ordered wavy step. Initially, the differential heat of adsorption is 95.11 kJ/mol, and the adsorption value is  $N = 0.57 H_2O/\text{ea}$ .

The main reason for the high heat of adsorption is that water molecules enter the zeolite cavities directly due to their small size, and high energies are generated by physical forces between oxygen atoms and adsorbate, which bind silicon and aluminum during the entry process. Then the heat of adsorption is reduced to  $\sim 13.5$  kJ/mol. In this process, it is adsorbed on  $Na^+$  cations in the SI position. After the heat reaches 81.65 kJ/mol, the heat difference transforms into a stepwise form. 2.29 water molecules are sorbed by cations 0.25  $Ca^{+2}$  and 0.25  $Na^+$  in position SIII. This phase is in the range from 81.65 kJ/mol to 77.62

kJ/mol, and the adsorption rate is in the range from 1.72 H<sub>2</sub>O/e to 4.01 H<sub>2</sub>O/e. For 3.47 molecules of water adsorption, the heat of adsorption decreases from 77.62 kJ/mol to 71.32 kJ/mol. 10.93 water molecules go through three stages to be adsorbed onto the zeolite.

At the same time, the difference in adsorption temperatures decreases to 71.32 kJ/mol, 68.50 kJ/mol, and 65.62 kJ/mol. It is known from the orderly decrease in adsorption temperatures that this means that the zeolite is adsorbed into a large cavity, that is, into the SII cavity. When the adsorption value reaches  $N = 22.44$  H<sub>2</sub>O/e, the temperature drops sharply to 54.46 kJ/mol. Here, the SII gap in the supervoids of the adsorbent indicates saturation. The main reason for the gradual abrupt decrease in the heat of adsorption from 77.62 kJ/mol is the formation of complex compounds with metal cations located in active centers in the zeolite's pores

In processes with a high heat of adsorption, it takes place in cavities SI and SIII. In the SII position of type A, the heat of adsorption decreases in the same wave-like linear form. At the end of the process, the heat of adsorption decreases from 53.17 kJ/mol to 50.42 kJ/mol, and then adsorption approaches the heat of condensation. The adsorption of Na<sup>+</sup> and Ca<sup>2+</sup> cations in the zeolite's pores ranges from 7.48 H<sub>2</sub>O/e.u. up to 22.77 H<sub>2</sub>O/e.e. At this stage, 15.29 H<sub>2</sub>O molecules/e.u. are adsorbed on Na<sup>+</sup> and Ca<sup>2+</sup> cations. In this case, multidimensional complexes (H<sub>2</sub>O) nNa<sup>+</sup> and (H<sub>2</sub>O) nCa<sup>2+</sup> are formed.

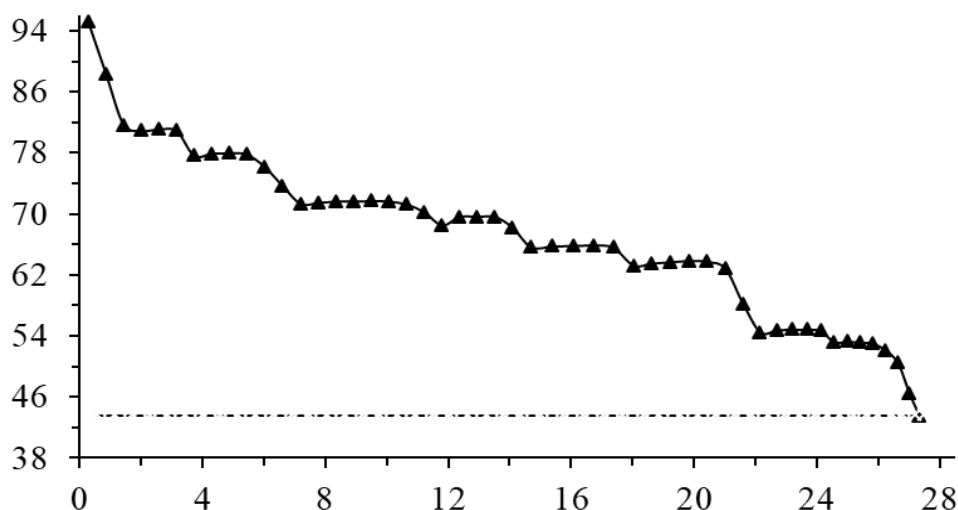


Figure 2. Differential heat of adsorption of water on zeolite Ca<sub>4</sub>Na<sub>4</sub>A at a temperature of 303 K. Horizontal annular heat condensation line

The pores of the Ca<sub>4</sub>Na<sub>4</sub>A zeolite have three adsorption slots, in which adsorbates will adsorbed. Alkali and alkaline earth metals form the basis of active centers. In the first cavity, Na<sup>2+</sup> cations are located in the center of the six-membered oxygen rings SI and form a b-cavity.

Since this cavity is small, it is partially saturated with metal cations. In the second cavity, the Ca<sup>2+</sup> and Na<sup>+</sup> cations are located slightly inside the plane of the eight-membered oxygen rings SII, and, finally, in the third cavity, the Ca<sup>2+</sup> and Na<sup>+</sup> SIII cations are located inside the large  $\alpha$ -cavity. opposite the four-membered oxygen ring.

It can be seen that cavities SIII and SII form the bulk of the adsorption as they are located within the space. This is due to the fact that the cations in the SI space are adsorbed in very small amounts because they are surrounded by cations of six strong protective oxygen atoms.

Ca<sub>4</sub>Na<sub>4</sub>A sorbs a total of 27.49 water molecules per zeolite. Of these, ~ 21.9 H<sub>2</sub>O e.ya. in the SII cavity and ~ 5 H<sub>2</sub>O e.ya. in the SIII cavity. In the SI space, 0.57 H<sub>2</sub>O is deposited.

Figure 3 shows the differential entropy of water adsorption on Ca<sub>4</sub>Na<sub>4</sub>A zeolite [35]. The formula of the Gibbs-Helmholtz equation was used to calculate the differential entropy using the differential heat and isotherm values of water adsorption on Ca<sub>4</sub>Na<sub>4</sub>A zeolite

$$\Delta S_d = \frac{\Delta H - \Delta G}{T} = \frac{-(Q_d - \lambda) + A}{T}$$

*T* – температура, *Q<sub>d</sub>* – ўртача дифференциал иссиқлик. *λ* – thermal condensation,  $\Delta H$  and  $\Delta G$  – enthalpy, and free energy change, *T* – temperature, *Q<sub>d</sub>* – average differential heat.

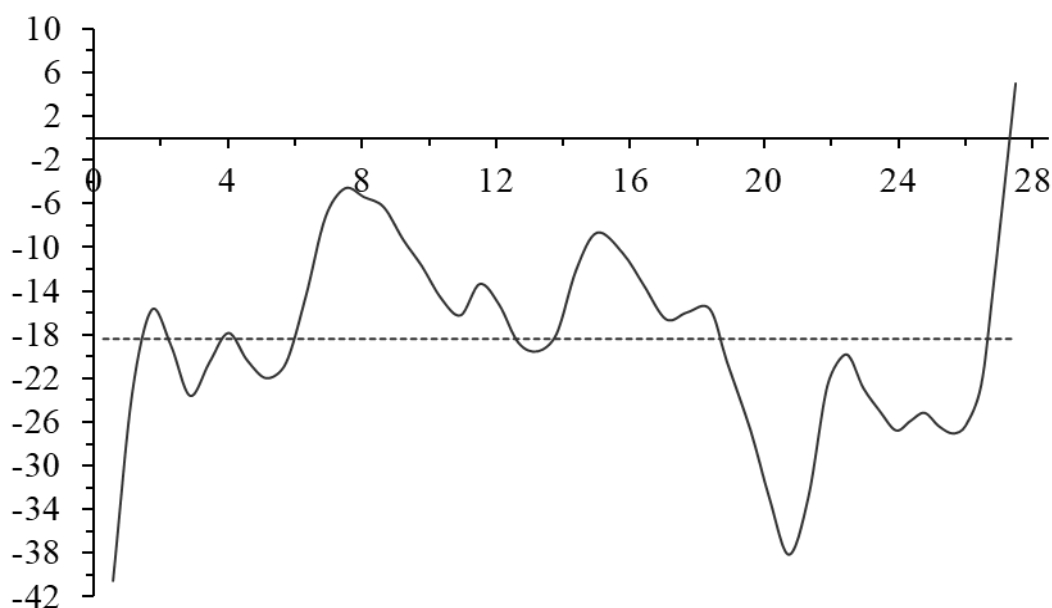


Figure 3. Differential entropy of water adsorption in Ca<sub>4</sub>Na<sub>4</sub>A zeolite is given

Based on the results of the study, the location of adsorbent voids, surface surfaces, and cations were studied in the study of adsorption entropy. It is known from the beginning of the process that the high adsorption heat indicates that the water molecules at the initial saturation are not strongly agitated in the zeolite micropores. The differential entropy of adsorption initially starts at -40.59 J/mol \* K, with adsorption N = 0.28 H<sub>2</sub>O e.ya. Then the entropy decreases to -15.74 J/mol\*K and increases to -23.58 J/mol\*K. Since there are many empty pores in this part of the zeolite, the adsorption entropy values will be high and the adsorbate molecules will be inactive because the cations are not completely saturated with water vapor. The differential entropy of adsorption has the form of waves in the range from N = 2.58 H<sub>2</sub>O e.ya to N = 16.74 H<sub>2</sub>O e.ya. e rises and falls to -15.64 J/mol\*K with wavy lines in four stages. The differential entropy of adsorption has the form of waves in the range from N = 2.58 H<sub>2</sub>O e.ya to N = 16.74 H<sub>2</sub>O e.ya. e rises and falls to -15.64 J/mol\*K with wavy lines in four stages. Then the adsorption of N ~ 27 H<sub>2</sub>O e.u. gradually appears from the average integral lines and approaches 0. This leads to the formation of complex compounds with Na<sup>+</sup> cations, which migrate from the SIII cavity into the SII cavity of the zeolite matrix, forming small wavy lines.

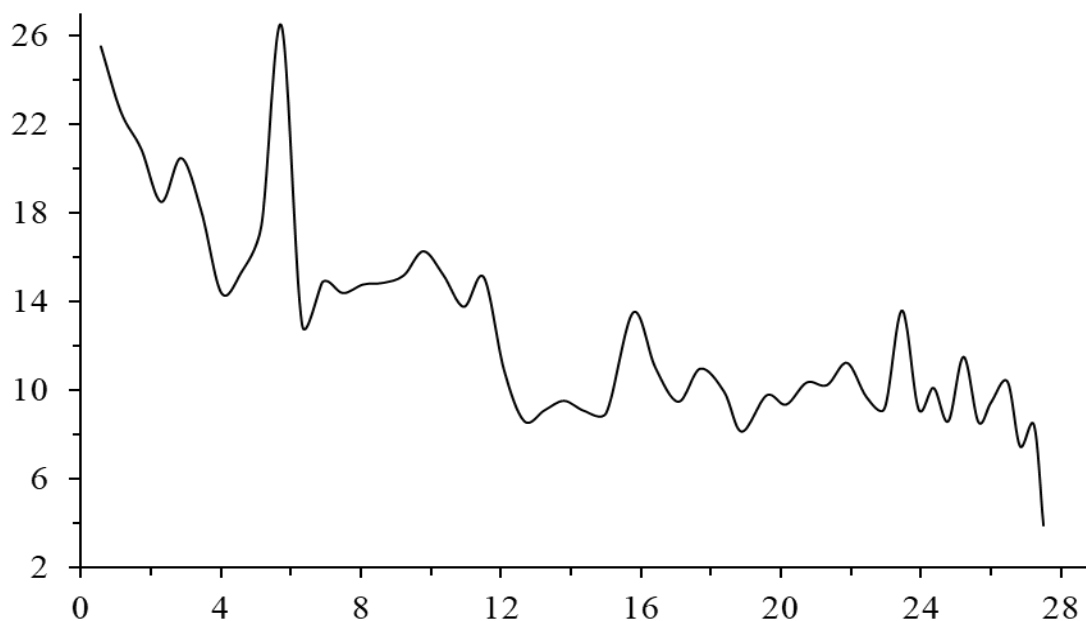


Figure 4. Time of equilibration of water adsorption in zeolite  $\text{Ca}_4\text{Na}_4\text{A}$ .

Due to a large number of cations in these cavities, the energy distribution during migration and adsorption of cations is ordered and strongly adsorbed. The average integral entropy is  $-18.39 \text{ J/mol}\cdot\text{K}$ .

In fig. 4 shows the equilibrium time of water adsorption on the  $\text{Ca}_4\text{Na}_4\text{A}$  zeolite. In this zeolite, the equilibrium timelines are in the form of strong waves.

The equilibrium time of water adsorption on the  $\text{Ca}_4\text{Na}_4\text{A}$  zeolite is initially 25.53 hours. Since at the initial saturation there are many voids in the micropores of the zeolite and, it takes more time to establish the equilibrium of water adsorption. In experiments, we take a small amount of adsorbate and absorb it into the sorbent. Due to a large number of cations in the pores of the zeolite and the lack of adsorbate in the pores and, the time required for the distribution of water molecules. In the processes, where a degree of adsorption is up to 12  $\text{H}_2\text{O}$  e.ya., the time of adsorption equilibrium is gradually reduced. After that, the equilibrium time gradually decreases sharply in the form of a smooth wave. At the end of the process, the equilibrium time was supported at  $\sim 3$  hours.

#### 4. CONCLUSION.

Based on the difference in heat and entropy of absorption in water vapor adsorbates were studied, the interactions between adsorbate-adsorbent and adsorbate-adsorbate due to adsorbent surfaces, microcapillary saturation, and capillary condensation. In  $\text{Ca}_4\text{Na}_4\text{A}$  zeolites, the heat of water adsorption takes the form of steps, where all steps form one- and multidimensional adsorption complexes  $(\text{H}_2\text{O}) n/\text{Ca}^+$  and  $(\text{H}_2\text{O}) n/\text{Na}^+$  in the matrix of  $\text{Ca}_4\text{Na}_4\text{A}$  zeolites. The adsorption isotherm is represented by the three-term *MXTN* equation. The total sorption volume of the  $\text{Ca}_4\text{Na}_4\text{A}$  zeolite is  $\sim 27.35 \text{ H}_2\text{O}/\text{e.u.}$  per unit cell. water molecule. Judging by the different values of entropy, water molecules are very strongly sorbed in these micropores of the zeolite. The average integral entropy of the differential entropy of adsorption is  $-18.39 \text{ J/mol}\cdot\text{K}$ . Water molecules are strongly adsorbed in the solid state in the supercavities of the zeolite. The adsorption of water on the  $\text{Ca}_4\text{Na}_4\text{A}$  zeolite

begins in 25.54 hours, at first it takes a very long time to reach the equilibrium time, and decreases to several hours (~ 3 hours) at the end of the process.

## 5. LIST OF USED LITERATURE.

- [ 1] ИВ.Г. Колобродов, В.Б.Кулько, Л.В.Карнацевич, Э.И.Винокуров, М.А. Хажмурадов, В.И.Жуковин, Н.В.Тимохина. Адсорбция и десорбция паров воды различными цеолитами // Вопросы атомной науки и техники, 2002. №1. С. 50-55.
- [ 2] Цеолит синтетический типа КА-БС. Технические условия. ТУ 2161-126-05766575-2005.
- [ 3] Sholl, D.; Lively, R., Seven chemical separations to change the world. Nature 2016, 532, 435–437.
- [ 4] Pera-Titus, M.; Palomino, M.; Valencia, S.; Rey, F. Thermodynamic analysis of framework deformation in Na,Cs-RHO zeolite upon CO<sub>2</sub> adsorption. Phys.Chem.Chem.Phys.2014, 16, 24391.
- [ 5] Lee, Y.; Reisner, B. A.; Hanson, J. C.; Jones, G. A.; Parise, J. B.; Corbin, D. R.; Toby, B. H.; Freitag, A.; Larese J. Z. New insight into cation relocations within the pores of zeolite rho: in situ synchrotron x-ray and neutron powder diffraction studies of Pb- and Cd-exchanged RHO. J. Phys. Chem. B 2001, 105, 7188-7199.
- [ 6] Lee, Y.; Hriljac, J. A.; Vogt, T.; Parise, J. B.; Edmondson, M. J.; Anderson, P. A.; Corbin, D. R.; Nagai, T. Phase transition of zeolite rho at high-pressure. J. Am. Chem. Soc. 2001, 123, 8418-8419.
- [ 7] Parise, J. B.; Gier, T. E.; Corbin, D. R.; Cox, D. E. Structural changes occurring upon dehydration of zeolite RHO. A study using neutron powder diffraction and distance-least-squares structural modelling. J. Phys. Chem. 1984, 88, 1635-1640.
- [ 8] Parise, J. B.; Corbin, D. R.; Abrams, L. Structural changes upon sorption and desorption of Xe from Cd-exchanged zeolite rho: a real-time synchrotron X-ray powder diffraction study. Microporous Mater. 1995, 4, 99-110.
- [ 9] Palomino, M.; Corma, A.; Jorda, J. L.; Rey F.; Valencia, S. Zeolite Rho: a highly selective adsorbent for CO<sub>2</sub>/CH<sub>4</sub> separation induced by a structural phase modification. Chem. Commun. 2012, 48, 215–217.
- [ 10] Ke, Q.; Sun, T.; Cheng, H.; Chen, H.; Liu, X.; Wei, X.; Wang, S. Targeted synthesis of ultrastable high-silica rho zeolite through alkali metal–crown ether interaction. Chem. Asian J. 2017, 12, 1043–1047.
- [ 11] Langmi, H.W.; Walton, A.; Al-Mamouri, M.M.; Johnson, S.R.; Book, D.; Speight, J.D.; Edwardsa, P.P.; Gameson, I.; Anderson, P.A.; Harris, I. R. Hydrogen adsorption in zeolites A, X, Y and RHO. J. Alloys Compd. 2003, 356, 710–715.
- [ 12] García-Sánchez, A.; Dubbeldam D.; Calero, S. Modeling adsorption and self-diffusion of methane in lta zeolites: the influence of framework flexibility J. Phys. Chem. C 2010, 114, 15068–15074.
- [ 13] Gymez-Blvarez, P.; Perez-Carbajo, J.; Balestra, S. R. G.; Calero, S. Impact of the nature of exchangeable cations on LTA-type zeolite hydration. J. Phys. Chem. C. 2016, 120, 23254–23261.
- [ 14] Bish, D. L.; Wang, H.-W. Phase transitions in natural zeolites and the importance of P<sub>H2O</sub>. Philosophical Magazine 2010, 90, 2425–2441.

- [ 15] T. F. Robin, A. B. Ross, A. R. Lea-Langton and J. M. Jones, Stability and activity of doped transition metal zeolites in the hydrothermal processing. *Front. Energy Res.* 2015, 3, 51.
- [ 16] Auroux, A. Microcalorimetry methods to study the acidity and reactivity of zeolites, pillared clays and mesoporous materials. *Top. Catal.* 2002, 19, 205–213.
- [ 17] Barrer, R. M.; Townsend, R. P. Transition metal ion exchange in zeolites. Part 1.—Thermodynamics of exchange of hydrated  $Mn^{2+}$ ,  $Co^{2+}$ ,  $Ni^{2+}$ ,  $Cu^{2+}$  and  $Zn^{2+}$  ions in ammonium mordenite. *J. Chem. Soc., Faraday Trans.* 1 1976, 72, 661-673.
- [ 18] Klier, K. Transition-metal ions in zeolites: the perfect surface sites. *Langmuir* 1988, 4, 13-25.
- [ 19] Balestra, S. R. G.; Hamad, S.; Ruiz-Salvador, A. R.; Domínguez-García, V.; Merkling, P. J.; Dubbeldam D.; Calero, S. Understanding nanopore window distortions in the reversible molecular valve zeolite RHO. *Chem. Mater.* 2015, 27, 5657–5667.
- [ 20] Wang, H.-W.; Bish, D.L. A  $PH_2O$ -dependent structural phase transition in the zeolite natrolite. *Am. Mineral.* 2008, 93, 1191.
- [ 21] Fridriksson, T.; Bish, D.L.; Bird, D.K. Hydrogen-bonded water in laumontite I: X-ray powder diffraction study of water site occupancy and structural changes in laumontite during room-temperature isothermal hydration/dehydration. *Am. Mineral.* 2003, 88, 277.
- [ 22] Cruciani, G.; Martucci, A.; Meneghini, C. Dehydration dynamics of epistilbite by in situ time resolved synchrotron powder diffraction. *Eur. J. Mineral.* 2003, 15, 257.
- [ 23] Rouquerol, J., Rouquerol, F., Llewellyn, P., Maurin, G. & Sing, K. S. Adsorption by powders and porous solids: principles, methodology and applications. (Academic press, 2013).
- [ 24] P.S. Kumar, S. Ramalingam, C. Senthamarai, M. Niranjanaa, P. Vijayalakshmi, S. Sivanesan, Adsorption of dye from aqueous solution by cashew nut shell: studies on equilibrium isotherm, kinetics and thermodynamics of interactions, *Desalination* 261 (1–2) (2010) 52–60.
- [ 25] K.Y. Foo, B.H. Hameed, Insights into the modeling of adsorption isotherm systems, *Chem. Eng. J.* 156 (2010) 2–10.
- [ 26] H. Aydin, G. Baysal, Adsorption of acid dyes in aqueous solutions by shells of bittimpistacial khinjuk stocks *Desalination* 196 (2006) 248–259.
- [ 27] M.B. Desta, Batch sorption experiments: Langmuir and Freundlich isotherm studies for the adsorption of textile metal ions onto Teff straw (*Eragrostis tef*) agricultural waste, *J. Thermodyn.* 375830 (2013) 6, <http://dx.doi.org/10.1155/2013/375830>.
- [ 28] K.V. Kumar, A. Kumaran, Removal of methylene blue by mango seed kernel powder, *Biochem. Eng. J.* 27 (2005) 83–93.
- [ 29] C. Namasivayam, R.T. Yamuna, Adsorption of Chromium(VI) by a low-cost adsorbent: biogas residual slurry, *Chemosphere* 30 (1995) 561–578.
- [ 30] N.K. Hamadi, X.D. Chen, M.M. Farid, G.M. Lu, Adsorption kinetics for the removal of chromium(VI) from aqueous solution by adsorptions derived from used tyres and sawdust, *Chem. Eng. J.* 84 (2001) 95–105.
- [ 31] B.F. Mentzen, G.U. Rakhmatkariev. Host/Guest interactions in zeolitic nanostructure MFI type materials: Complementarily of X-ray Powder Diffraction, NMR spectroscopy, Adsorption calorimetry and Computer Simulations // *Узб. хим. журнал.* 2007, №6, С. 10-31.



- [ 32] U. Rakhmatkariev. Mechanism of Adsorption of Water Vapor by Muscovite: A Model Based on Adsorption Calorimetry // Clays and Clay Minerals, 2006 vol. 54. pp. 423-430.
- [ 33] 33. Рахматкариев Г.У., Исирикян А.А. Полное описание изотерм адсорбции уравнениями теории объемного заполнения микропор // Изв. АН СССР. Сер.хим. -1988. -№11. -С. 2644.
- [ 34] 34. Dubinin M.M. Progress in Surface Membrane Science. -New York, 1975. -Vol. 9. - P. 1-70.
- [ 35] 35. Рахматкариева Ф.Г., Рахматкариев Г.У. Ион-молекулярные комплексы в наноструктурированных цеолитах NaA и NaA(NaBO<sub>2</sub>) // Узбекский химический журнал, 2016, №4. - С.3-9.